Lithium Fast-Ionic Conduction in Complex Hydrides: Review and Prospects

*Motoaki Matsuo and Shin-ichi Orimo**

Complex hydrides exhibit various energy-related functions such as hydrogen storage, microwave absorption, and neutron shielding. Furthermore, another novel energy-related function was recently reported by the authors; lithium fast-ionic conduction, which suggests that complex hydrides may be a potential candidate for solid electrolytes in lithium-ion batteries. This review presents the recent progress in the development of lithium fast-ionic conductors of complex hydrides. First, the fast-ionic conduction in $LiBH_4$ as a result of clarifying the mechanism of microwave absorption is presented, and then the conceptual development of complex hydrides as a new type of solid-state lithium fast-ionic conductors in $LiBH_4$–, $LiNH_2$–, and $LiAlH_4$-based complex hydrides is discussed. Finally, the future prospects of this study from both application and fundamental viewpoints are described: possible use as solid electrolytes for batteries, formation of ionic liquids in complex hydrides, and similarity between complex hydrides and Laves-phase metal hydrides.

1. Introduction

Complex hydrides are generally denoted by $MM'H_n$, where M is a metal cation and $M'H_n$ represents a complex anion such as $[BH_4]^-$, $[NH_2]^-$, $[AlH_4]^-$, $[NH]^{2-}$, $[AlH_6]^{3-}$, or $[NiH_4]^{4-}$.[1,2] Complex hydrides with the $[BH_4]^-$ anion are called borohydrides or tetrahydroborates. Experimental and theoretical investigations of various borohydrides with M cation(s) (M: Li, Na, K, Mg, Sc, Cu, Zn, Zr, or Hf) have been systematically conducted to clarify their stability; the results reveal that charge compensation by the M cation is essential for achieving optimum stability of all borohydrides.[3–6]

$LiBH_4$ (lithium borohydride or lithium tetrahydroborate) is a representative complex hydride with ionic bonding between the Li^+ and $[BH_4]^-$ complex ions; its crystal structures[7–9] are shown in **Figure 1**. At room temperature (RT), the hydride crystallizes in an orthorhombic structure with space group *Pnma* [low-temperature (LT) phase; Figure 1a]. Each Li^+ ion is surrounded by four $[BH_4]^-$ ions in a tetrahedral configuration. At approximately 390 K, the structure undergoes a structural transition and becomes hexagonal with space group $P6_3mc$ [high-temperature (HT) phase; Figure 1b]. Apart from its classical application as a reducing agent or a precursor for the synthesis of organometallic derivatives, $LiBH_4$ has attracted considerable interest as a potential candidate for an advanced hydrogen storage material. $LiBH_4$ can release large amounts of hydrogen by the following desorption reaction above 600 K:[10–12]

$$LiBH_4 \rightarrow LiH + B + 3/2H_2 \quad (1)$$

To improve the kinetics of reaction (1), the self-heating of $LiBH_4$ caused by microwave irradiation was investigated. There was a significant enhancement in self-heating above the structural transition temperature of 390 K, which resulted in rapid hydrogen desorption above 600 K.[13,14] This phenomenon triggered the discovery of lithium fast-ionic conduction in $LiBH_4$[15] because permittivity measurements suggested that the self-heating of $LiBH_4$ was due to conductive loss,[13] although $LiBH_4$ acts as an electrical insulator in both LT and HT phases with a large band gap of approximately 7 eV.[3,16]

The search for and development of lithium fast-ionic conductors are important because of the potential applications of such materials as solid electrolytes to improve the safety- and energy-density-related issues of conventional lithium-ion batteries.[17–21] However, only a few reports regarding lithium ionic conduction in complex hydrides were published although a wide variety of inorganic lithium fast-ionic conductors[22–25] such as oxides,[26–29] nitride,[30] sulfides,[31–34] and LiI-based composites[35,36] was reported. Bureau et al. investigated the electrical conductivity of Li_3AlH_6 and Na_3AlH_6, and concluded

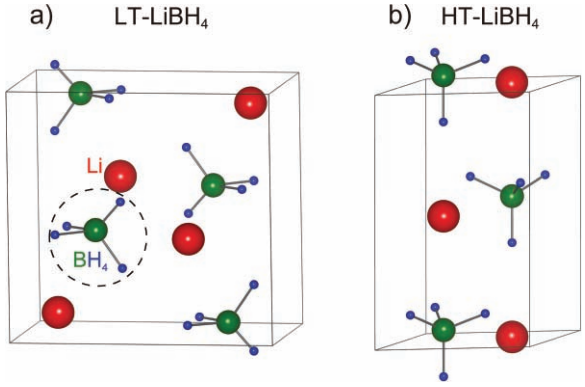

Figure 1. Crystal structures of the a) LT and b) HT phases of $LiBH_4$.[7–9]

Prof. S. Orimo, Dr. M. Matsuo
Institute for Materials Research
Tohoku University
Katahira 2–1–1, Sendai, 980–8577 Japan
E-mail: orimo@imr.tohoku.ac.jp

DOI: 10.1002/aenm.201000012

that the former is an insulator (neither an electronic nor an ionic conductor) and the latter an electronic conductor.[37] Lithium fast-ionic conduction in complex hydrides was first reported for Li_2NH, composed of Li^+ and $[NH]^{2-}$ complex ions, by Boukamp and Huggins in 1979.[38] Li_2NH exhibits fast-ionic conductivity of 3×10^{-4} S cm^{-1} at RT. However, no further study regarding Li_2NH was conducted until Araújo et al. very recently approached it using ab initio molecular-dynamics simulation,[39] because of the limited practical applications of Li_2NH due to its low electrochemical stability of 0.7 V. No complex hydride has since been found to be a lithium fast-ionic conductor. Therefore, it is fundamentally and practically significant to investigate lithium ionic conduction in $LiBH_4$. Herein, we first present the lithium fast-ionic conduction in $LiBH_4$ and then discuss the conceptual development of complex hydrides as a new category of solid-state lithium fast-ionic conductors. Finally, the future prospects of this new category of conductors are discussed.

2. Lithium Fast-Ionic Conduction in $LiBH_4$

We predicted that $LiBH_4$ can act as an ionic conductor, and further, that the carrier is not a H^+ ion but a Li^+ ion because hydrogen atoms are covalently stabilized as $[BH_4]^-$ complex ions. In this section, we first describe the experimental investigations into the electrical conductivity and dynamics of Li^+ ions in $LiBH_4$ by using an AC complex impedance method and ^{7}Li NMR spectroscopy, respectively.[15] We then discuss the possible mechanism of fast-ionic conduction on the basis of a high-pressure experiment and a computational approach. We also address the electrochemical stability required for possible applications.

2.1. Discovery

Figure 2 shows the electrical properties of $LiBH_4$. The impedance plots of both the LT and HT phases show only a single arc (Figure 2a), which indicates that a response arising from grain boundaries is not observed even though the pelletized sample used for impedance measurement was simply prepared by pressing powdered $LiBH_4$ without subsequent sintering. As shown in Figure 2b, the conductivities of the LT phase are very low, between 10^{-8} and 10^{-6} S cm^{-1}, and they increase linearly with temperature. At approximately 390 K, that is, the transition temperature, the conductivity increases drastically by three orders of magnitude. As a result, the HT phase exhibits high conductivity, on the order of 10^{-3} S cm^{-1}. The activation energies for conduction are evaluated as 0.69 eV and 0.53 eV for the LT and HT phases, respectively.

To confirm whether the high electrical conductivity of $LiBH_4$ in the HT phase is due to the fast mobility of Li^+ ions, ^{7}Li NMR measurements were performed. **Figure 3** shows the ^{7}Li NMR spectra at selected temperatures. The shapes of the spectra change drastically at the structural transition temperature. In the LT phase (below 385 K), only small, broad peaks are observed. On the contrary, in the HT phase (above 388 K), each spectrum shows a central sharp line and two satellite lines. The decrease in the line width of the central line indicates motional narrowing caused by lithium fast-ionic motion in the HT phase. The temperature dependence of the spin-lattice relaxation time T_1 was also investigated, as shown in **Figure 4**. The value of T_1 increases with temperature and then decreases steeply at approximately 390 K. These NMR features were also confirmed by Skripov et al.[40,41] and Corey et al.[42] after our report.

The NMR-derived conductivity in the HT phase can be estimated using the correlation times of the lithium ionic motion obtained from the T_1 curve above 390 K. Clearly, the NMR data agree fairly well with the measured electrical conductivities, as shown in Figure 2b. Furthermore, the DC conductivity measurements showed that electronic conduction was almost negligible. Thus, we can conclude that the high electrical conductivity on the order of 10^{-3} S cm^{-1} in the HT phase is a result of the fast mobility of Li^+ ions and that $LiBH_4$ is a lithium fast-ionic conductor.

2.2. Possible Mechanism

The ^{7}Li NMR measurements suggest possible two-dimensional diffusion in the HT phase of $LiBH_4$. The NMR-derived conductivity using a two-dimensional factor agrees better with the

Motoaki Matsuo received his Ph.D. in materials science in 2008 from Tohoku University. He worked as a postdoctoral fellow in 2008–2010, and is currently an assistant professor in the Orimo group of the Institute for Materials Research, Tohoku University. His research interests are fundamental, physical, and chemical properties of light-weight hydrides, particularly solid-state ionics and hydrogen storage.

Shin-ichi Orimo received his Ph.D. in materials science/physics from Hiroshima University in 1995. He was a JSPS research fellow (1993–1995), a research associate in Hiroshima University (1995–2002), and a guest researcher at the Max-Planck Institute for Metal Research for which he was funded by an Alexander von Humboldt Fellowship and a MEXT Fellowship (1998–1999). He is now a professor of the Institute for Materials Research, Tohoku University. His research interests are fundamentals and energy-related applications of hydrides, particularly hydrogen storage and solid-state ionics.

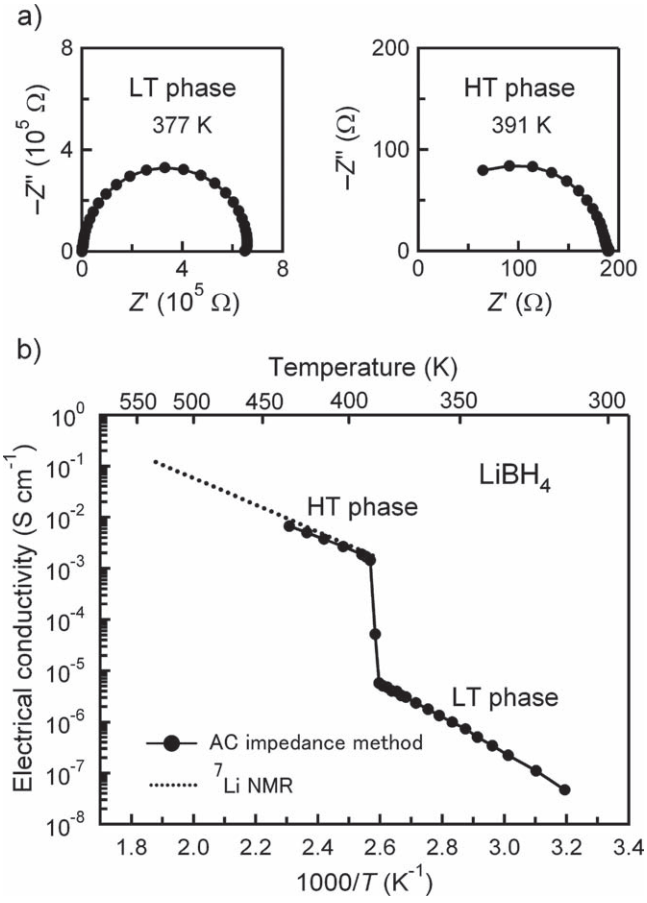

Figure 2. Electrical properties of $LiBH_4$ measured in a heating run. a) Typical impedance plots obtained using a lithium-metal electrode at 377 K (LT phase) and 391 K (HT phase). b) Arrhenius plots of the electrical conductivities. The ^7Li NMR-derived conductivity is also shown (dotted line).[15]

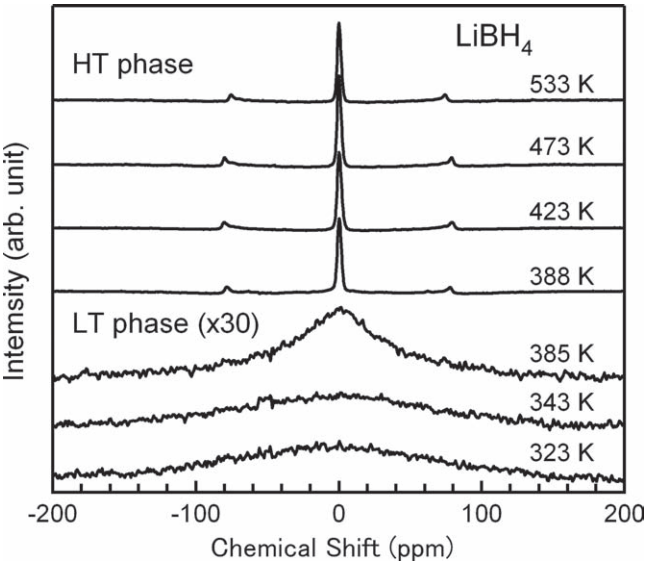

Figure 3. ^7Li NMR spectra of $LiBH_4$ at selected temperatures. Reproduced with permission from ref. [15]. Copyright 2007 American Institute of Physics.

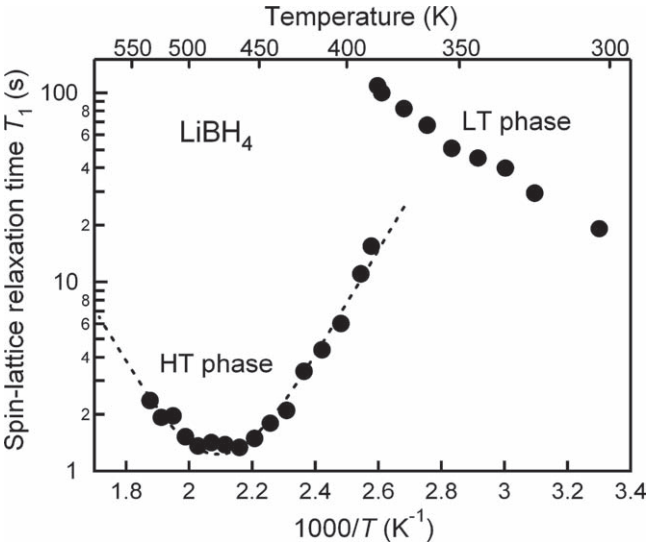

Figure 4. Temperature dependence of the spin-lattice relaxation time T_1 of $LiBH_4$. Reproduced with permission from ref. [15]. Copyright 2007 American Institute of Physics.

measured conductivity than that derived using a one- or three-dimensional factor.[15] Epp and Wilkening also confirmed the low-dimensional diffusion feature by using temperature- and frequency-dependent NMR spectroscopy.[43] The characteristic feature of the HT structure is that both Li^+ and $[BH_4]^-$ ions line up along the *a* and *b* axes such that there is no $[BH_4]^-$ ion between Li^+ ions and vice versa.[7–9] This arrangement may enable Li^+ ions to migrate along the *a* and *b* axes.

High-pressure (2–6 GPa) AC impedance measurements at various temperatures showed that the activation volume for ionic conduction was around 3 $cm^3\ mol^{-1}$ for the HT phase (corresponding to approximately $0.09V_m$, where V_m is the molar volume).[44] This value is almost comparable to the activation volume for other fast-ionic conductors such as α-AgI,[45] $La_{0.52}Li_{0.35}TiO_{2.96}$,[46] and NASICONs.[47] This result implies that a sufficient number of interstitial sites into which Li^+ ions can jump are intrinsically built into the structure, as reported for Li_3N,[30] Li_2NH,[39] and Li_3PO_4.[48]

Moreover, by using first-principles molecular-dynamics simulations, it has been demonstrated that double splitting of the lithium occupation in the original lithium site plays an important role in creating a metastable interstitial site surrounded by three Li^+ ions and three $[BH_4]^-$ ions in the *a*–*b* plane and a connection path between the two closest Li sites.[49]

Another aspect of the mechanism, interactions between the fast mobility of Li^+ ions and the dynamics of $[BH_4]^-$ ions,[50–52] is strongly anticipated. Rotational motion of the translationally static $[BH_4]^-$ anions can enhance the mobility of Li^+ ions, as discussed for Li_2SO_4 in a paddle-wheel mechanism in which the transport of Li^+ ions strongly correlates with the rotation of the SO_4 tetrahedra.[53] We experimentally confirmed that the activation energy for hydrogen reorientational motion in $[BH_4]^-$ anions (0.69 eV), obtained by ^1H NMR spectroscopy, agrees well with that for the lithium ionic conduction (0.67 eV) in the $LiBH_4$–LiBr system.[54]

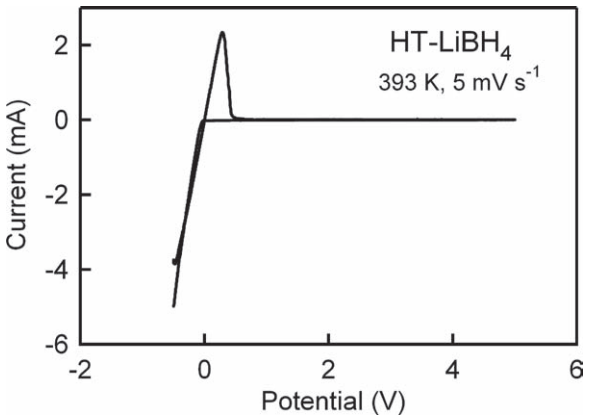

Figure 5. Cyclic voltammograms of $LiBH_4$ sandwiched between the lithium and molybdenum electrodes taken at 390 K with a voltage scan rate of 5 mV s^{-1}.

2.3. Electrochemical Stability

As a potential candidate for solid electrolytes in all-solid-state lithium-ion batteries, $LiBH_4$ must have high electrochemical stability. **Figure 5** shows the cyclic voltammograms of the HT phase of $LiBH_4$ sandwiched between lithium and molybdenum electrodes. Only cathodic and anodic currents are observed near 0 V (vs. Li^+/Li), which correspond to lithium deposition on the molybdenum electrode and lithium dissolution, respectively. No significant anodic currents caused by hydride decomposition are observed up to at least 5 V (vs. Li^+/Li), which indicates a reasonably large electrochemical window.

3. Lithium Fast-Ionic Conduction in $LiBH_4$-Based Complex Hydrides

Lithium fast-ionic conduction in $LiBH_4$ could potentially contribute to the development of solid electrolytes in all-solid-state batteries. For this application, however, it is highly desirable to enhance the conductivity at RT. To achieve this, we now present our recent conceptual material development of fast-ion conductors of $LiBH_4$-based complex hydrides.

3.1. $LiBH_4$–Li*X* (*X* = Cl, Br and I) System

We assumed that stabilization of the HT phase should significantly improve the conductivity at RT, and that replacing $[BH_4]^-$ complex ions with I^- ions, whose ionic radius (0.220 nm) is larger than that of the $[BH_4]^-$ ion (0.205 nm),[55] will effectively improve the stability because alkali-metal borohydrides MBH_4 (*M* = Na, K, Rb, and Cs) with longer distances between neighboring $[BH_4]^-$ ions have been reported to exhibit lower transition temperatures.[56] Therefore, we systematically investigated the structural and thermodynamic properties and the conductivity of the $LiBH_4$–LiI system.[54,57,58]

Figure 6 shows the powder X-ray diffraction (XRD) profiles of $(1–x)LiBH_4 + xLiI$ synthesized by mechanical milling under Ar atmosphere.[57] Only the diffraction peaks corresponding to the LT or HT phase are observed for all *x*, which indicates that all samples are single-phase. The diffraction peak intensities of the LT phase of $LiBH_4$ decrease drastically when $x = 0.06$. The HT phase can be detected when $x = 0.25$ and 0.50; this indicates stabilization of the HT phase of $LiBH_4$ at RT. In addition, no diffraction peaks originating from the superlattice formation are observed, and the lattice constants of the HT phase ($x = 0$, 0.25, and 0.50) increase with *x*. These results indicate the formation of $Li(BH_4–I)$ solid solutions by the replacement of $[BH_4]^-$ ions with I^- ions, similar to Li(Br–I) in the LiBr–LiI system.[59]

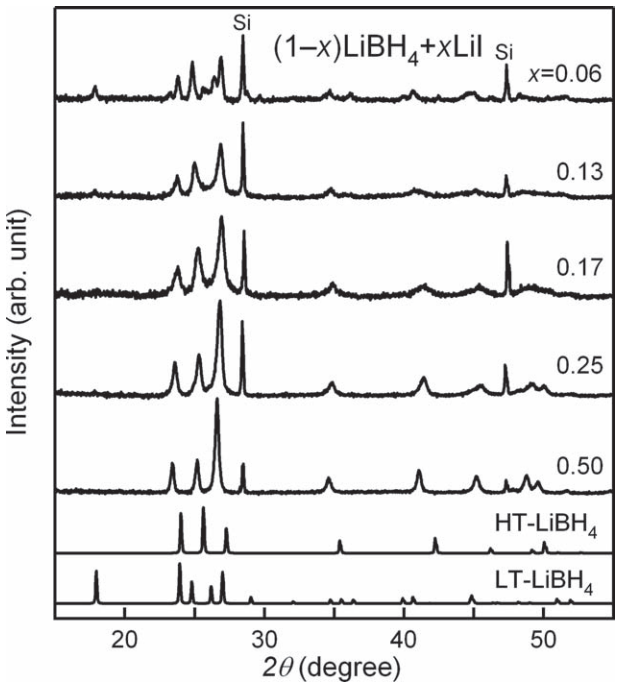

Figure 6. Powder XRD profiles of $(1–x)LiBH_4 + xLiI$ (x = 0.06–0.50). The diffraction peaks are calibrated using a Si internal standard. The standard diffraction peaks of the LT and HT phases of $LiBH_4$ are shown for reference.[7] Reproduced with permission from ref. [57]. Copyright 2009 American Institute of Physics.

The thermodynamic properties of the $LiBH_4$–LiI system were examined using differential scanning calorimetry (DSC) and the results are shown in **Figure 7**a.[57] The endothermic peaks directly correspond to the structural transition. Both the peak temperatures (onset) and enthalpy changes (areas) decrease until $x = 0.17$. No endothermic peak is detected for $x > 0.25$, which indicates that the HT phase is stabilized at RT. Note that no change is observed in the DSC profiles for $x = 0.25$ even after 10 and 20 heating/cooling cycles (heating up to 423 K and cooling down to RT); such cyclic stability is preferable for solid electrolytes.

The structural transition temperatures obtained from Figure 7a are plotted as a function of *x*, as shown in **Figure 7b**. We can confirm the stabilization feature of the HT phase depending on the molar ratio of LiI. Recent studies have indicated that simultaneous rotations of $[BH_4]^-$ ions and lattice anharmonicity

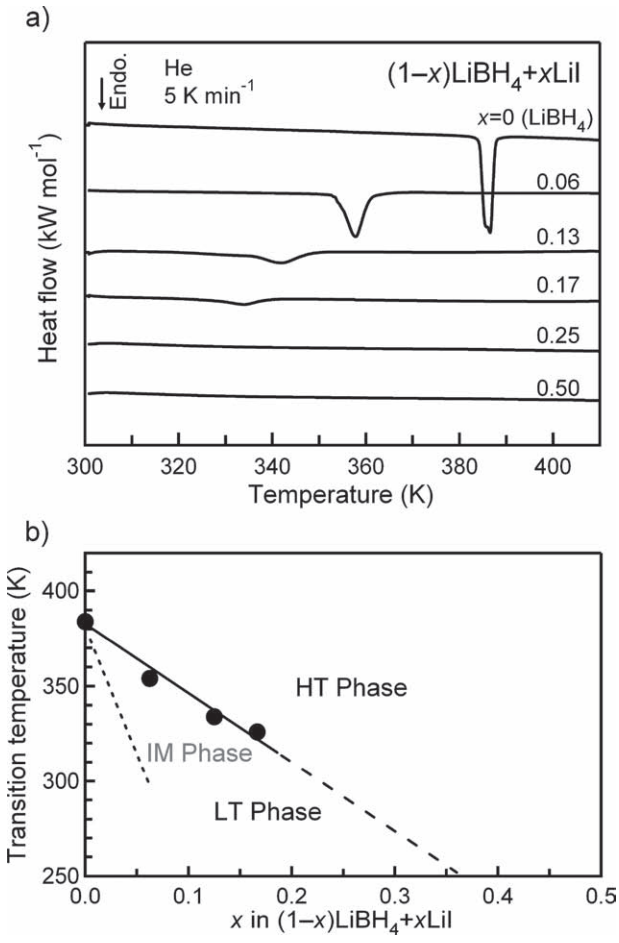

Figure 7. a) DSC profiles of $(1-x)LiBH_4 + xLiI$ ($x = 0.06–0.50$). The intensities are normalized to show the heat flow per mole of the formula unit of $(1-x)LiBH_4 + xLiI$. b) Structural transition temperatures of $(1-x)LiBH_4 + xLiI$ as a function of x. The intermediate (IM) phases are predicted for $x = 0.06–0.17$. Reproduced with permission from ref. [57]. Copyright 2009 American Institute of Physics.

strongly affect the structural transition of $LiBH_4$.[60–62] In fact, spatially resolved Raman spectroscopy demonstrates the importance of anharmonic effects on the structural transformation in this system.[63]

Figure 8 shows the ionic conductive properties of $(1-x)LiBH_4 + xLiI$.[54,58] The change in the activation energy due to the structural transition is observed at around 340 K for $x = 0.13$, whereas the conductivities for $x = 0.25$ exhibit Arrhenius behavior throughout the measured temperature range because of HT phase stabilization. As expected, the conductivity at RT increases by three orders of magnitude without a decrease in the high conductivity of the HT phase. Furthermore, the activation energy decreases with LiI content due to faster mobility of Li^+ ions caused by the high polarizability of I^- ions substituted for $[BH_4]^-$ ions.[64] The minimum value for the activation energy is obtained for $x = 0.13$ (0.39 eV),[58] as also suggested by the ^7Li NMR T_1 measurement.[54] We also confirmed that the replacement of $[BH_4]^-$ ions with Cl^- or Br^- ions enhances the conductivity.[54,65]

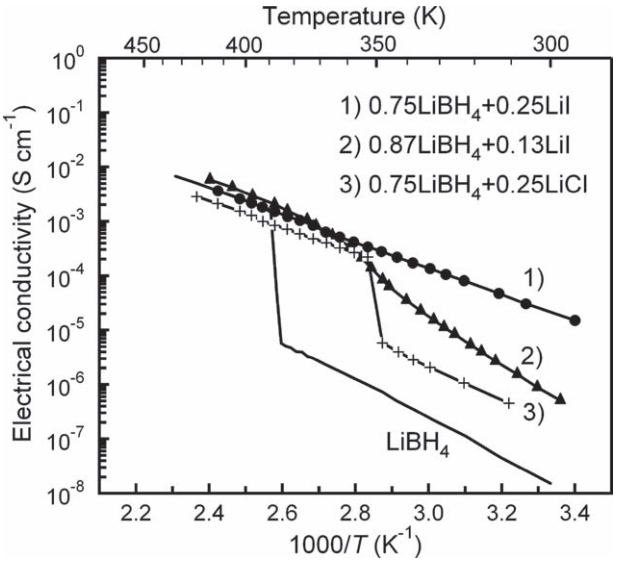

Figure 8. Temperature dependence of the electrical conductivities measured in a heating run of $(1-x)LiBH_4 + xLiX$ (X = Cl and I).[54,58,65] Data for $LiBH_4$ is also shown for reference.[15]

3.2. $LiBH_4$–$LiNH_2$ System

The $LiBH_4$–$LiNH_2$ system has been studied in terms of developing hydrogen storage materials, and two phases, $Li_2(BH_4)(NH_2)$ and $Li_4(BH_4)(NH_2)_3$, are known to exist.[66–72] As shown in **Figure 9**, both $Li_2(BH_4)(NH_2)$ and $Li_4(BH_4)(NH_2)_3$ have

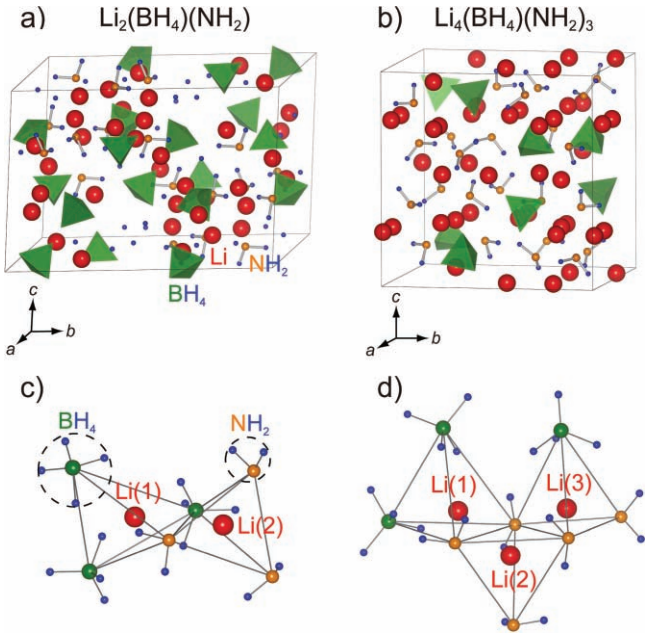

Figure 9. a), b) Crystal structures of $Li_2(BH_4)(NH_2)$ and $Li_4(BH_4)(NH_2)_3$.[66–72] c), d) Multiple occupation sites for Li^+ ion in the hydrides. Reproduced with permission from ref. [73]. Copyright 2009 American Chemical Society.

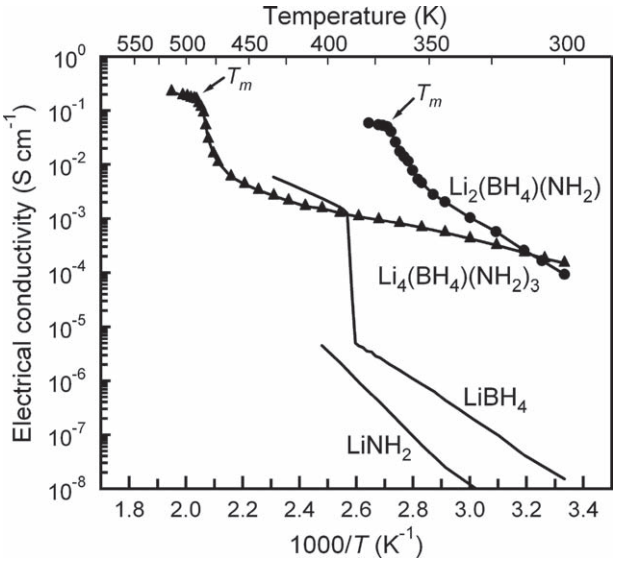

Figure 10. Temperature dependences of the electrical conductivities measured in a heating run of $Li_2(BH_4)(NH_2)$ and $Li_4(BH_4)(NH_2)_3$.[73] The melting temperatures (365 K for $Li_2(BH_4)(NH_2)$ and 490 K for $Li_4(BH_4)(NH_2)_3$) are indicated as T_m. For reference, the data for $LiBH_4$[15] and $LiNH_2$ are also shown.

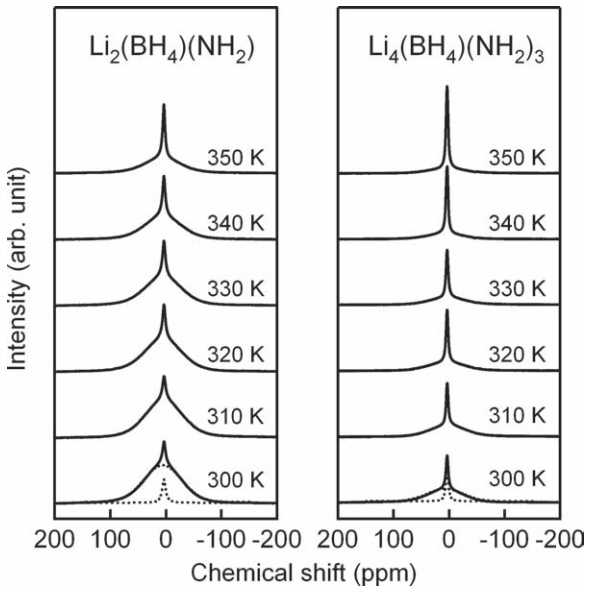

Figure 11. ^{7}Li NMR spectra of (left) $Li_2(BH_4)(NH_2)$ and (right) $Li_4(BH_4)(NH_2)_3$ at selected temperatures measured in a heating run. Reproduced with permission from ref. [73]. Copyright 2009 American Chemical Society.

different anion configurations from $LiBH_4$. In these cases, Li^+ ions are tetrahedrally coordinated by combinations of $[BH_4]^-$ and $[NH_2]^-$ complex ions. The $LiBH_4$–LiI system shows that the ionic conductivity is significantly affected by the anion configuration, which increased our interest in these local structures. Moreover, $Li_2(BH_4)(NH_2)$ and $Li_4(BH_4)(NH_2)_3$ melt at temperatures around 360 K and 460 K,[69] respectively, indicating possible enhancement of the total ionic conductivity at these temperatures. Therefore, we investigated the conductivities of $Li_2(BH_4)(NH_2)$ and $Li_4(BH_4)(NH_2)_3$ before and after melting.[73]

As shown in **Figure 10**, $Li_2(BH_4)(NH_2)$ exhibits fast-ionic conductivity of 1×10^{-4} S cm^{-1} even at RT, which is four and five orders of magnitude higher than those of the host hydrides $LiBH_4$ (LT phase) and $LiNH_2$, respectively. Moreover, the conductivity increases monotonically upon heating. The activation energy for conduction decreases significantly at around 368 K from 0.66 eV (303–348 K) to 0.24 eV (above 368 K) as a result of the melting of $Li_2(BH_4)(NH_2)$. The total ionic conductivity reaches 6×10^{-2} S cm^{-1} after melting at the highest temperature measured, 378 K. This result suggests that $Li_2(BH_4)(NH_2)$ could be used as an ionic liquid as well as a solid-state fast-ionic conductor, as will be discussed in Section 5.2. $Li_4(BH_4)(NH_2)_3$ also shows high conductivity of 2×10^{-4} S cm^{-1} at RT, and the conductivity value reaches 2×10^{-1} S cm^{-1} at 513 K, after melting. Furthermore, the activation energy for conduction before melting is determined to be 0.26 eV. It is noteworthy that this value is less than half the value in $Li_2(BH_4)(NH_2)$ before melting and $LiBH_4$ (LT phase: 0.69 eV; HT phase: 0.53 eV), which indicates that $Li_4(BH_4)(NH_2)_3$ has higher Li^+ ion mobility than that of $Li_2(BH_4)(NH_2)$ or $LiBH_4$.

This fast mobility was also confirmed by ^{7}Li NMR; the results are shown in **Figure 11**. A narrowing of the line widths is observed even at RT for both $Li_2(BH_4)(NH_2)$ and $Li_4(BH_4)(NH_2)_3$, which indicates the fast mobility of Li^+ ions in these complex hydrides at RT. The overlapping of a broad Gaussian component and a sharp Lorentzian component suggest the existence of Li^+ ions with low mobility as well as those with high mobility, which can be attributed to the local atomistic structures of the hydrides.

Both $Li_2(BH_4)(NH_2)$ and $Li_4(BH_4)(NH_2)_3$ have multiple occupation sites for Li^+ ions (Figures 9c and 9d). $Li_2(BH_4)(NH_2)$ has eighteen Li(1)s and eighteen Li(2)s per unit cell, whereas $Li_4(BH_4)(NH_2)_3$ has twelve Li(1)s, twelve Li(2)s, and eight Li(3)s. The radius of each occupation site, which could be a qualitatively suitable factor for estimating the bottleneck size for lithium ionic diffusion, is as follows: In $Li_2(BH_4)(NH_2)$, Li(1) = 0.16 nm and Li(2) = 0.09 nm, and in $Li_4(BH_4)(NH_2)_3$, Li(1) = 0.17 nm, Li(2) = 0.11 nm, and Li(3) = 0.11 nm. Note that in $Li_2(BH_4)(NH_2)$, 50% of the Li^+ ions occupy the rather small Li(2) site [approximately 56% of the radius and 18% of the volume of Li(1)]. $Li_2(BH_4)(NH_2)$ has a higher ratio for the peak areas of the Gaussian against Lorentzian components and a larger activation energy for conduction than $Li_4(BH_4)(NH_2)_3$ because of the Li^+ ions with lower mobility at Li(2). Because of its low melting temperature $Li_2(BH_4)(NH_2)$ nevertheless exhibits as high conductivity at RT as $Li_4(BH_4)(NH_2)_3$. The disordered structure at around the melting temperature enhances carrier concentration.

4. Lithium Ionic Conduction in Other Complex Hydrides

As mentioned in the Introduction, various complex hydrides other than $LiBH_4$ exist. Investigations into lithium ionic conduction in these hydrides can be highly beneficial for

establishing appropriate research directions for enhancing lithium ionic conductivities in complex hydrides. Here, we report the results of our investigations into $LiNH_2$-based and $LiAlH_4$-based complex hydrides.

4.1. $LiNH_2$-Based Complex Hydrides

The results from the $LiBH_4$–LiI and $LiBH_4$–$LiNH_2$ systems suggest that similar fast-ionic conductors may exist in the $LiNH_2$–LiI system, although neither $LiNH_2$[73] nor LiI[35] exhibits high ionic conductivity. Hence, samples were synthesized by mechanical milling across various compositions, and the crystal structures as well as the conductive properties were characterized in detail.[74]

Powder XRD profiles of $(1–x)LiNH_2$+ xLiI (x = 0.06–0.75) obtained using our laboratory X-ray apparatus (Lab-XRD), shown in **Figure 12**a, exhibit diffraction peaks originating from a new phase along with those from the starting material $LiNH_2$ or LiI, over the entire range of composition ratios. The peak positions of the new phase are unshifted for all values of x, which indicates that the new phase may be a stoichiometric compound. Only the new phase appears to be detected for $x = 0.25$.

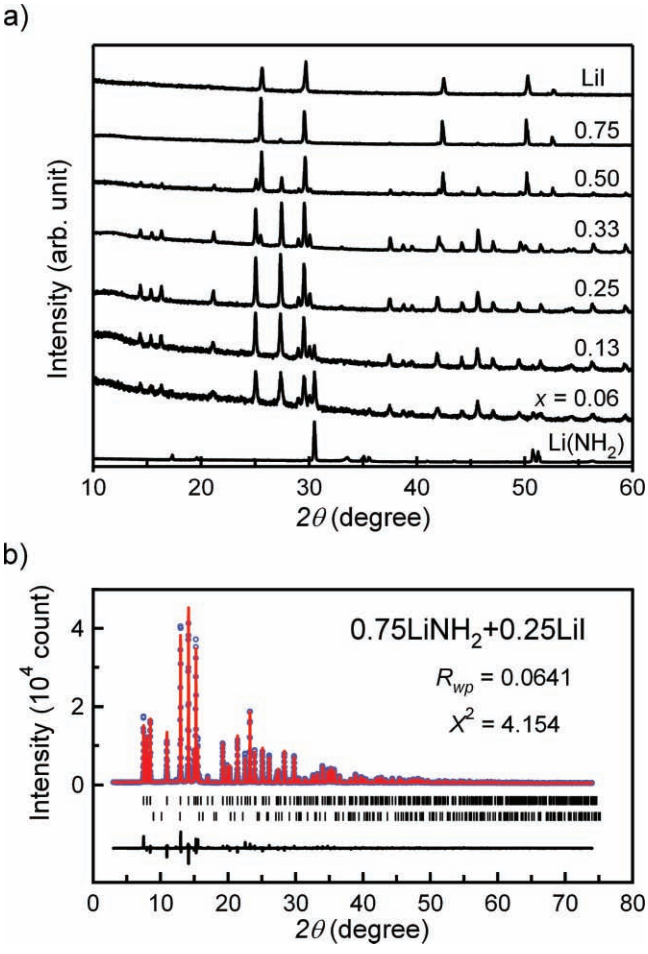

Figure 12. a) Lab-XRD profiles of $(1– x)LiNH_2$+ xLiI (x = 0.06–0.75). For reference, the data of $LiNH_2$ and LiI as host materials are also shown. b) Rietveld refinement fits of SR-XRD for $0.75LiNH_2$ + 0.25LiI. The observed, calculated, and difference between observed and calculated profiles are indicated as blue circles, a red line, and a black line, respectively. The positions of Bragg reflection are shown for $Li_3(NH_2)_2I$ (upper) and $LiNH_2$ (lower). Reproduced with permission from ref. [74]. Copyright 2010 American Chemical Society.

To determine the crystal structure of the new phase, a high-resolution synchrotron powder XRD experiment was conducted for x = 0.25 at RT (SR-XRD, λ = 0.08006 nm). The Rietveld refinement of the SR-XRD for the new phase is shown in Figure 12b. The Figure demonstrates that small peaks of unreacted $LiNH_2$ exist, and that the new phase is a complex hydride $Li_3(NH_2)_2I$ with a = 0.709109(5) nm, c = 1.150958(10) nm, space group $P6_3mc$ (hexagonal), and Z = 4.

The crystal structure of $Li_3(NH_2)_2I$ is illustrated in **Figure 13**. The Li atoms are located at two crystallographically different positions [Li(1) and Li(2)]. Both Li(1) and Li(2) atoms are tetrahedrally coordinated by three N atoms ($[NH_2]^-$ complex ions) and one I atom [tetrahedra T1 for Li(1) and T2 for Li(2)]. The primary structural feature is clusters of three T1 and three T2 tetrahedra, which share their edges with each other. The double-layered structure consists of corner-sharing clusters such that the upper layer forms an angle of 60° with the lower.

Figure 14 shows the temperature dependences of the conductivity for x = 0.06, 0.13, and 0.25. For all values of x, the conductivities exhibit Arrhenius behavior throughout the measured temperature range. The maximum conductivity of 2×10^{-5} S cm^{-1} at 300 K, which is four and three orders of magnitude higher than those of the host materials $LiNH_2$ and LiI, respectively, is obtained for x = 0.25 of all compositions, although almost equimolar $LiNH_2$ exists in the sample. This result implies that higher conductivity can be achieved for single-phase $Li_3(NH_2)_2I$. The activation energy for conduction is determined to be 0.58 eV, which is comparable to that of the HT phase of $LiBH_4$ (0.53 eV).

The lithium fast-ionic conduction in $Li_3(NH_2)_2I$ is probably closely related to its unique crystal structure. As shown in Figure 13, many intrinsic interstitial sites appear at the center of the cluster of six tetrahedra and between the clusters. Li^+ ions may migrate through these spaces.

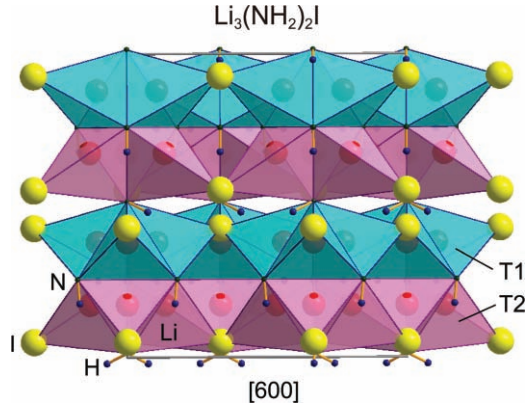

Figure 13. Crystal structure of the new complex hydride $Li_3(NH_2)_2I$ viewed along [600]. T1 and T2 indicate tetrahedra composed of three N atoms and one I atom for Li(1) and Li(2), respectively.[74]

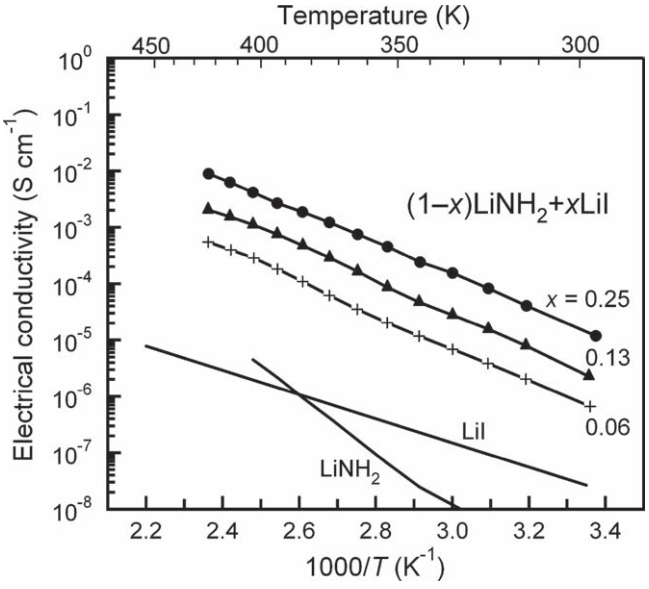

Figure 14. Temperature dependences of the electrical conductivities measured in a heating run of of $(1–x)LiNH_2 + xLiI$ (x = 0.06, 0.13, and 0.25).[74] For reference, the data for $LiNH_2$[73] and LiI[35] as host materials are also shown.

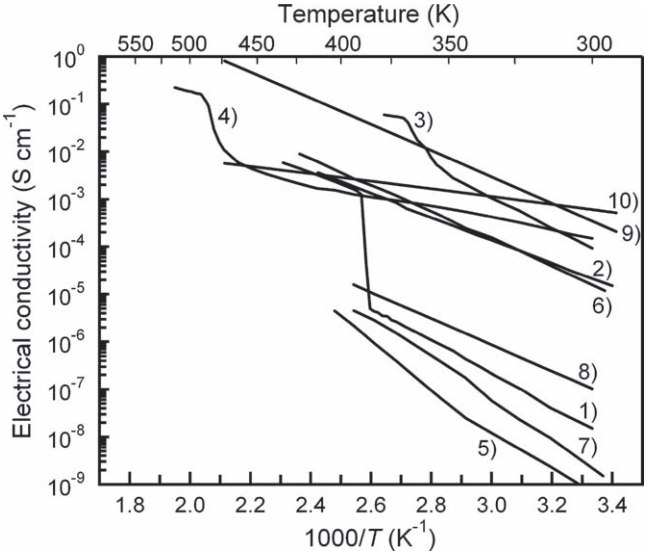

Figure 15. Summarized lithium ionic conductivities of complex hydrides: 1) $LiBH_4$,[15] 2) $Li(BH_4)_{0.75}I_{0.25}$ ($LiBH_4$–LiI system),[54,58] 3),4) $Li_2(BH_4)(NH_2)$ and $Li_4(BH_4)(NH_2)_3$ ($LiBH_4$–$LiNH_2$ system),[73] 5),6) $LiNH_2$ and $Li_3(NH_2)_2I$ ($LiNH_2$-based complex hydrides),[74] and 7),8) $LiAlH_4$ and Li_3AlH_6 ($LiAlH_4$-based complex hydrides).[80] For reference, the data of related compounds are also shown: 9) Li_2NH[38] and 10) Li_3N.[35]

Another feature of the structure, its similarity with Laves-phase metal hydrides, will be presented in Section 5.3.

4.2. $LiAlH_4$-Based Complex Hydrides

$LiAlH_4$ and Li_3AlH_6 are complex hydrides that exhibit ionic bonding between the Li^+ ion and the $[AlH_4]^-/[AlH_6]^{3-}$ complex ion. Similar to $LiBH_4$, these complex hydrides behave as electrical insulators with a wide bandgap.[75–77] However, the crystal structures, coordination number of Li^+ cations, ionic radii, and anion valences of these hydrides differ from those of $LiBH_4$.[78,79] In this section, we describe our investigations into lithium ionic conduction in $LiAlH_4$ and Li_3AlH_6.[80]

The conductivities of $LiAlH_4$ and Li_3AlH_6 are shown in **Figure 15**. The temperature dependence of the conductivities of $LiAlH_4$ and Li_3AlH_6 exhibits Arrhenius behavior; the conductivities increase almost linearly from 2×10^{-9} to 5×10^{-6} S cm^{-1} for $LiAlH_4$ and from 1×10^{-7} to 2×10^{-5} S cm^{-1} for Li_3AlH_6. The activation energies of $LiAlH_4$ and Li_3AlH_6 are 0.76 and 0.61 eV, respectively. These values are comparable with the activation energy of the LT phase of $LiBH_4$ (0.69 eV). We can conclude that Li_3AlH_6 is a lithium ionic conductor although Bureau et al. have reported that Li_3AlH_6 is an insulator[37] as described in the Introduction.

To improve the ionic conductivity of Li_3AlH_6, Li_3AlH_6–LiX (X = Cl and I) systems were investigated. In particular, the Li_3AlH_6–LiI system ($0.75Li_3AlH_6 + 0.25LiI$) exhibits superior conductive properties; the conductivity at RT increases by thirty-five times over that of Li_3AlH_6 and the activation energy also significantly decreases to 0.48 eV from 0.61 eV. XRD measurements revealed that LiI partially dissolved into Li_3AlH_6. The better conductive properties can be attributed to the substitution of $[AlH_6]^{3-}$ with I^-; a more polarizable anion sublattice, as observed for the $LiBH_4$–LiI system, causes faster mobility of Li^+ ions and lithium vacancies formed by the aliovalent substitution lead to increased carrier concentration.[64]

5. Prospects

Further research and developments can be expected to yield practical applications of these materials as solid electrolytes for batteries and also to demonstrate new phenomena that are characteristic of complex hydrides. Future prospects are discussed briefly below.

5.1. Possible Application of Complex Hydrides as Solid Electrolytes

$LiBH_4$ has not only high ionic conductivity but also the following advantages as a solid electrolyte in lithium-ion batteries: 1) negligible electronic conductivity, 2) extremely low grain-boundary resistance, 3) high electrochemical stability up to at least 5 V (vs. Li^+/Li) at 390 K, 4) high stability to chemical reaction with elemental Li and graphite-based anodes, 5) commercial availability, and 6) suitability for various material processes (mechanical milling, impregnation,[81] and vapor deposition). On the other hand, problems regarding sensitivity to moisture and reactivity with oxide cathode electrodes must be overcome.

Non-oxide cathode materials must be developed because complex hydrides have a relatively strong reducing ability. We are designing materials consisting of lithium-containing borides, carbides, and boro-carbides with layered structures. One

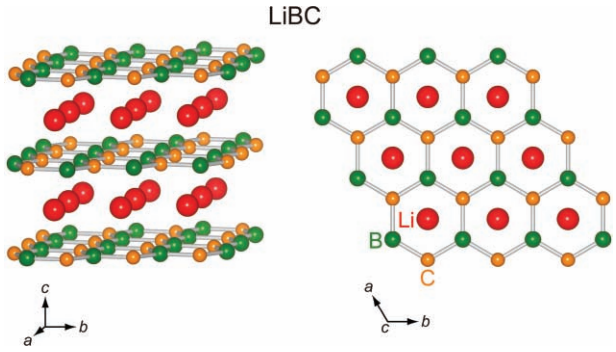

Figure 16. Crystal structure of LiBC [$a = 0.27523(3)$ nm, $c = 0.7058(2)$ nm, space group $P6_3mmc$, and $Z = 2$].[82,83]

promising candidate is LiBC, with a hexagonal structure of alternating graphene BC and Li layers, as shown in **Figure 16**,[82,83] which has been attracting considerable interest as a possible superconductor because it is isoelectronic with MgB_2.[84–88] LiBC has advantages in terms of not only low reactivity with complex hydrides but also capacity due to its light-weight constituent elements. If Li^+ ions can be reversibly extracted from the crystal structure of LiBC, as shown in the following reaction, a significantly high capacity (for example, 450 mAh g^{-1} for $x = 0.5$) may theoretically be obtained. We have successfully synthesized single-phase $Li_{0.5}BC$.[89]

$$LiBC \leftrightarrow xLi^+ + Li_{1-x}\,BC + xe \quad (2)$$

Additionally, our group is focusing on the synthesis of thin-film LiBH4 by using melting, vapor deposition, or pulsed laser deposition to demonstrate all-solid-state batteries using complex-hydride solid electrolytes.[90] Thin-film LiBH4 would enable the fabrication of thin-film lithium-ion batteries[91] such as graphite/thin-film LiBH4/above-mentioned new cathode for a microelectromechanical system, MEMS.[92–95]

5.2. Formation of Ionic Liquid in Complex Hydrides

Various ionic liquids, which are organic liquid salts at, or close to, RT, have been proposed as a novel class of ionic conductive materials for electrochemical applications such as polymer-electrolyte-membrane fuel cells, lithium-ion batteries, and supercapacitors.[96]

As described in Section 3.2, both $Li_2(BH_4)(NH_2)$ and $Li_4(BH_4)(NH_2)_3$ have relatively low melting temperatures. In particular, $Li_2(BH_4)(NH_2)$ melts below 373 K and exhibits a high conductivity of 6×10^{-2} S cm^{-1} after melting. To our knowledge, there are no reports of inorganic lithium fast-ionic conductors with such low melting temperatures. Our results suggest that $Li_2(BH_4)(NH_2)$ could be a candidate for the first application of an inorganic compound as an ionic liquid. For the optimum use of $Li_2(BH_4)(NH_2)$ as an ionic liquid in electrochemical applications, details of the phase-separation reaction including desorption of a small amount of ammonia,[63] ion-transport properties,[97] and electrochemical stability of molten $Li_2(BH_4)(NH_2)$ must be clarified. Using Raman spectroscopy, we confirmed that both $[BH_4]^-$ and $[NH_2]^-$ complex anions remain intact even after melting. Further systematic studies by NMR and cyclic voltammetry are in progress.

5.3. Similarity Between Complex Hydrides and Laves-Phase Metal Hydrides

In Section 4.1, the characteristic layered structure of the new complex hydride $Li_3(NH_2)_2I$ was described. In this section, we additionally note the similarity between the crystal structures of $Li_3(NH_2)_2I$ and the Laves-phase metal hydrides.

Laves-phase compounds, that is, intermetallic compounds with the ideal composition AB_2, consist of close-packed structures with ideal atomic size ratio $R_A/R_B = 1.225$ (in practice, numerous compounds are formed over the range 1.05–1.68)[98] and are classified into three structural types on the basis of their crystal-structure geometry: hexagonal $MgZn_2$ (C14), cubic $MgCu_2$ (C15), or hexagonal $MgNi_2$ (C36). The hydrogen desorption/absorption properties of the Laves-phase metal hydrides have been extensively investigated for effective application as hydrogen storage materials.

Among the three types of structures, we focus on the C14-type Laves-phase metal hydrides. **Figure 17** compares the crystal structures of $Li_3(NH_2)_2I$ and a representative C14-type Laves-phase metal hydride (deuteride) $ZrMn_2D_3$ [$a = 0.54055(9)$ nm, $c = 0.87964(7)$ nm, space group $P6_3mmc$, and $Z = 4$].[99] Interestingly, I^- and $[NH_2]^-$ ions have configurations similar to those of Zr and Mn atoms, respectively. The ionic radius ratio R_I/R_{NH2} of 1.31 (0.220 nm for I^- and 0.168 nm for $[NH_2]^-$),[55] which agrees well with the above-mentioned range 1.05–1.68, appears to be an important contributing factor to the Laves-phase-related structure; some electronic factors such as the valence electron concentration and electronegativity also affect the formation of Laves-phase structures.

To date, complex hydrides and metal hydrides have been regarded as different classes of materials, and few common guidelines for material development have been obtained (for example, with respect to hydrogen storage properties).

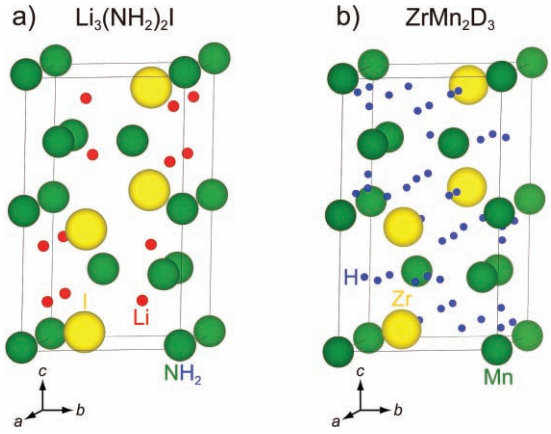

Figure 17. Crystal structures of a) $Li_3(NH_2)_2I$[70] and b) C14-type Laves-phase metal hydride $ZrMnD_3$.[99] For convenient comparison, $[NH_2]^-$ ions are displayed as green balls. Li, NH_2, and I in $Li_3(NH_2)_2I$ correspond to D, Mn, and Zr in $ZrMnD_3$, respectively.

Table 1. Crystal structures and lithium ionic conductivities of complex hydrides.

Complex Hydride	Crystal Structure		$\sigma_{300\,K}$ [a]	E_a [b]	Ref.
	Lattice Constant [nm]	Space Group	[S cm^{-1}]	[eV]	
$LiBH_4$ (HT phase)	$a = 0.427631(5)$ $c = 0.694844(8)$	$P6_3mc$ (Hexagonal)	1×10^{-3} (393 K)	0.53	[7], [15]
$LiBH_4$ (LT phase)	$a = 0.717858(4)$ $b = 0.443686(2)$ $c = 0.680321(4)$	$Pnma$ (Orthorhombic)	2×10^{-8}	0.69	
$Li(BH_4)_{0.75}I_{0.25}$	$a = 0.4354(2)$ $c = 0.7035(5)$	$P6_3mc$ (Hexagonal)	2×10^{-5}	0.48	[54], [57], [58]
$Li_2(BH_4)(NH_2)$	$a = 1.43944(3)$ $c = 0.90522(3)$	R-3 (Trigonal)	1×10^{-4}	0.66	[72], [73]
$Li_4(BH_4)(NH_2)_3$	$a = 1.06645(1)$	$I2_13$ (Cubic)	2×10^{-4}	0.26	[72], [73]
$LiNH_2$	$a = 0.504309(7)$ $c = 1.02262(3)$	I-4 (Tetragonal)	4×10^{-10}	0.94	[73], [100]
$Li_3(NH_2)_2I$	$a = 0.709109(5)$ $c = 1.150958(10)$	$P6_3mc$ (Hexagonal)	2×10^{-5}	0.58	[74]
$LiAlH_4$	$a = 0.48254(1)$ $b = 0.78040(1)$ $c = 0.78968(1)$	$P2_1/c$ (Monoclinic)	2×10^{-9}	0.76	[78], [80]
Li_3AlH_6	$a = 0.807117(10)$ $c = 0.95130(2)$	R-3 (Trigonal)	1×10^{-7}	0.61	[79], [80]
Li_2NH	$a = 0.50742(2)$	Fm-3m (Cubic)	3×10^{-4}	0.58	[38], [101]
Li_3N	$a = 0.36529(2)$ $c = 0.38736(2)$	$P6/mmm$ (Hexagonal)	7×10^{-4} [c]	0.25 [c]	[30], [100]

[a] Lithium ionic conductivity at 300 K;
[b] Activation energy for ionic conduction; [c] Data for polycrystalline Li_3N.

Therefore, we expect that $Li_3(NH_2)_2I$ may be the first good example of a bridge between complex hydrides and metal hydrides, which will lead to significant breakthroughs in the development of materials with superior lithium ionic conductive and hydrogen storage properties.

6. Conclusions

Herein, we first presented the discovery of lithium fast-ionic conduction in $LiBH_4$ as a result of clarifying the mechanism of hydrogen desorption by microwave irradiation. We then discussed the conceptual development of complex hydrides as a new category of solid-state lithium fast-ionic conductors in $LiBH_4$-based, $LiNH_2$-based, and $LiAlH_4$-based complex hydrides (summarized in **Table 1**). Finally, we described the future prospects of this study from both application and fundamental viewpoints. These prospects include possible use as solid electrolytes for batteries, as potential candidate for the first inorganic compound used as an ionic liquid, and the similarity between the crystal structures of complex hydrides and Laves-phase metal hydrides as the first example of bridging the different classes of hydrides. Therefore, the research topics presented in this paper should be worthy of further investigation in the future.

Acknowledgements

We gratefully acknowledge financial support received from the Japanese Ministry of Education, Culture, Sports, Science and Technology (KAKENHI No. 22760529 and 21246100); the International Collaboration Center, Institute for Materials Research (ICC-IMR). Valuable collaboration and communication with the groups of Prof. A. Züttel, Dr. A. Borgschulte, and Dr. A. Remhof of EMPA, Switzerland; Dr. T. Vegge of Risø National Laboratory for Sustainable Energy, Denmark; Prof. W. I. F. David, Dr. M. O. Jones, and Dr. S. Callear of ISIS, UK; Prof. T. Otomo and Dr. K. Ikeda of High Energy Accelerator Research Organization; Prof. H. Maekawa, Prof. H. Takamura, Dr. H. Oguchi, Dr. T. Sato, Dr. S. Semboshi, Dr. H.-W. Li, Mr. Y. Zhou, Mr. R. Miyazaki, and Ms. H. Ohmiya of Tohoku University are highly appreciated.

Received: October 28, 2010
Revised: December 3, 2010
Published online: January 20, 2011

[1] S. Orimo, Y. Nakamori, J. R. Eliseo, A. Züttel, C. M. Jensen, *Chem. Rev.* **2007**, *107*, 4111.
2] C. Liu, F. Li, L.-P. Ma, H.-M. Cheng, *Adv. Mater.* **2010**, *22*, E28.
[3] K. Miwa, N. Ohba, S. Towata, Y. Nakamori, S. Orimo, *Phys. Rev. B* **2004**, *69*, 245120.
[4] K. Miwa, N. Ohba, S. Towata, Y. Nakamori, S. Orimo, *J. Alloys Compd.* **2005**, *404–406*, 140.
[5] Y. Nakamori, K. Miwa, H.-W. Li, A. Ninomiya, N. Ohba, S. Towata, A. Züttel, S. Orimo, *Phys. Rev. B* **2006**, *74*, 045126.
[6] Y. Nakamori, H.-W. Li, K. Kikuchi, M. Aoki, K. Miwa, S. Towata, S. Orimo, *J. Alloys Compd.* **2007**, *446–447*, 296.
[7] J.-P. Soulié, G. Renaudin, R. Cerny, K. Yvon, *J. Alloys Compd.* **2002**, *346*, 200.
[8] M. R. Hartman, J. J. Rush, T. J. Udovic, R. C. Bowman Jr., S.-J. Hwang, *J. Solid State Chem.* **2007**, *180*, 1298.
[9] Y. Filinchuk, D. Chernyshov, R. Cerny, *J. Phys. Chem. C* **2008**, *112*, 10579.
[10] D. S. Stasinevich, G. A. Egorenko, *Russ. J. Inorg. Chem.* **1968**, *13*, 341.
[11] A. Züttel, P. Wenger, S. Rentsch, P. Sudan, Ph. Mauron, C. Emmenegger, *J. Power Sources* **2003**, *118*, 1.
[12] A. Züttel, S. Rentsch, P. Fischer, P. Wenger, P. Sudan, Ph. Mauron, Ch. Emmenegger, *J. Alloys Compd.* **2003**, *356–357*, 515.
[13] Y. Nakamori, S. Orimo, T. Tsutaoka, *Appl. Phys. Lett.* **2006**, *88*, 112104.

[14] M. Matsuo, Y. Nakamori, K. Yamada, S. Orimo, *Appl. Phys. Lett.* **2007**, *90*, 232907.
[15] M. Matsuo, Y. Nakamori, S. Orimo, H. Maekawa, H. Takamura, *Appl. Phys. Lett.* **2007**, *91*, 224103.
[16] E. Orgaza, A. Membrilloa, R. Castañeda, A. Aburtob, *J. Alloys Compd.* **2005**, *404–406*, 176.
[17] N. Machida, H. Maeda, H. Peng, T. Shigematsu, *J. Electrochem. Soc.* **2002**, *149*, A688.
[18] M. Tatsumisago, F. Mizuno, A. Hayashi, *J. Power Sources* **2006**, *159*, 193.
[19] N. Ohta, K. Takada, L. Zhang, R. Ma, M. Osada, T. Sasaki, *Adv. Mater.* **2006**, *18*, 2226.
[20] T. Kobayashi, Y. Imade, D. Shishihara, K. Homma, M. Nagao, R. Watanabe, T. Yokoi, A. Yamada, R. Kanno, T. Tatsumi, *J. Power Sources* **2008**, *182*, 621.
[21] F. M. Oudenhoven, L. Baggetto, P. H. L. Notten, *Adv. Ener. Mater.* **2011**, *1*, 10.
[22] G. Adachi, N. Imanaka, H. Aono, *Adv. Mater.* **1996**, *8*, 127.
[23] A. D. Robertson, A. R. West, A. G. Ritchie, *Solid State Ionics* **1997**, *104*, 1.
[24] P. Knauth, H. L. Tuller, *J. Am. Chem. Soc.* **2002**, *85*, 1654.
[25] P. Knauth, *Solid State Ionics* **2009**, *180*, 911.
[26] H. Aono, E. Sugimoto, Y. Sadaoka, N. Imanaka, G. Adachi, *J. Electrochem. Soc.* **1993**, *140*, 1827.
[27] Y. Inaguma, C. Liquan, M. Itoh, T. Nakamura, T. Uchida, H. Ikuta, M. Wakihara, *Solid State Commun.* **1993**, *86*, 689.
[28] A. Martínez-Juárez, J. M. Rojo, J. E. Iglesias, J. Sanz, *Chem. Mater.* **1995**, *7*, 1857.
[29] V. Thangadurai, W. Weppner, *Adv. Func. Mater.* **2005**, *15*, 107.
[30] A. Rabenau, *Solid State Ionics* **1982**, *6*, 277.
[31] M. Tachez, J. P. Malugani, R. Mercier, G. Robert, *Solid State Ionics* **1987**, *14*, 181.
[32] K. Takada, N. Aotani, K. Iwamoto, S. Kondo, *Solid State Ionics* **1996**, *86–88*, 877.
[33] R. Kanno, M. Murayama, *J. Electrochem. Soc.* **2001**, *148*, A742.
[34] F. Mizuno, A. Hayashi, K. Tadanaga, M. Tatsumisago, *Adv. Mater.* **2005**, *17*, 918.
[35] C. C. Liang, *J. Electrochem. Soc.* **1973**, *120*, 1289.
[36] H. Maekawa, R. Tanaka, T. Sato, Y. Fujimaki, T. Yamamura, *Solid State Ionics* **2004**, *175*, 281.
[37] J. C. Bureau, Z. Amri, P. Claudy, J. M. Létoffé, B. Balland, *Mat. Res. Bull.* **1989**, *24*, 1989.
[38] B. A. Boukamp, R. A. Huggins, *Phys. Lett. A* **1979**, *72*, 464.
[39] C. M. Araújo, A. Blomqvist, R. H. Scheicher, P. Chen, R. Ahuja, *Phys. Rev. B* **2009**, *79*, 172101.
[40] A. V. Skripov, A. V. Soloninin, Y. Filinchuk, D. Chernyshov, *J. Phys. Chem. C* **2008**, *112*, 18701.
[41] A. V. Soloninin, A. V. Skripov, A. L. Buzlukov, A. P. Stepanov, *J. Solid State Chem.* **2009**, *182*, 2357.
[42] R. L. Corey, D. T. Shane, R. C. Bowman Jr., M. S. Conradi, *J. Phys. Chem. C* **2008**, *112*, 18706.
[43] V. Epp, M. Wilkening, *Phys. Rev. B* **2010**, *82*, 020301.
[44] H. Takamura, Y. Kuronuma, H. Maekawa, M. Matsuo, S. Orimo, *Solid State Ionics*, in press.
[45] B.-E. Mellander, *Phys. Rev. B* **1982**, *26*, 5886.
[46] Y. Inaguma, J. Yu, Y.-J. Shan, M. Itoh, T. Nakamura, *J. Electrochem. Soc.* **1995**, *142*, L8.
[47] G. A. Samara, *Solid State Phys.* **1984**, *38*, 1.
[48] Y. A. Du, N. A. W. Holzwarth, *Phys. Rev. B* **2007**, *76*, 174302.
[49] T. Ikeshoji, E. Tsuchida, K. Ikeda, M. Matsuo, H.-W. Li, Y. Kawazoe, S. Orimo, *Appl. Phys. Lett.* **2009**, *95*, 221901.
[50] H. Hagemann, S. Gomes, G. Renaudin, K. Yvon, *J. Alloys Comp.* **2004**, *363*, 126.
[51] F. Buchter, Z. Łodziana, Ph. Mauron, A. Remhof, O. Friedrichs, A. Borgschulte, A. Züttel, D. Sheptyakov, Th. Strässle, A. Ramirez-Cuesta, *Phys. Rev. B* **2008**, *78*, 094302.
[52] A. Remhof, Z. Łodziana, P. Martelli, O. Friedrichs, A. Züttel, A. V. Skripov, J. P. Embs, T. Strässle, *Phys. Rev. B* **2010**, *81*, 214304.
[53] A. Lundén, *Solid State Commun.* **1988**, *65*, 1237.
[54] H. Maekawa, M. Matsuo, H. Takamura, M. Ando, Y. Noda, T. Karahashi, S. Orimo, *J. Am. Chem. Soc.* **2009**, *131*, 894.
[55] D. R. Lide, in *CRC Handbook of Chemistry and Physics*, 88th Ed., (Ed: D. R. Lide), CRC press, Boca Raton, FL **2007**.
[56] C. C. Stephensen, D. W. Rice, W. H. Stockmayer, *J. Chem. Phys.* **1955**, *23*, 1960.
[57] H. Oguchi, M. Matsuo, J. S. Hummelshøj, T. Vegge, J. K. Nørskov, T. Sato, Y. Miura, H. Takamura, H. Maekawa, S. Orimo, *Appl. Phys. Lett.* **2009**, *94*, 141912.
[58] R. Miyazaki, T. Karahashi, N. Kumatani, Y. Noda, M. Ando, H. Takamura, M. Matsuo, S. Orimo, H. Maekawa, *Solid State Ionics*, in press.
[59] J. Sangster, A. D. Pelton, *J. Phys. Chem.* **1987**, *16*, 509.
[60] Y. Filinchuk, D. Chernyshov, R. Cerny, *J Phys. Chem. C* **2008**, *112*, 10579.
[61] F. Buchter, Z. Łodziana, Ph. Mauron, A. Remhof, O. Friedrichs, A. Borgschulte, A. Züttel, *Phys. Rev. B* **2008**, *78*, 094302.
[62] A.-M. Racu, J. Schoenes, Z. Łodziana, A. Borgschulte, A. Züttel, *J. Phys. Chem. A* **2008**, *112*, 9716.
[63] A. Borgschulte, R. Gremaud, S. Kato, P. Stadie, A. Remhof, A. Züttel, M. Matsuo, S. Orimo, *Appl. Phys. Lett.* **2010**, *97*, 031916.
[64] A. R. West, in*Solid State Electrochemistry*, (Ed: P. G. Bruce), Cambridge University Press, Cambridge **1995**.
[65] M. Matsuo, H. Takamura, H. Maekawa, H.-W. Li, S. Orimo, *Appl. Phys. Lett.* **2009**, *94*, 084103.
[66] T. Noritake, M. Aoki, S. Towata, A. Ninomiya, Y. Nakamori, S. Orimo, *Appl. Phys. A* **2006**, *83*, 277.
[67] P. A. Chater, W. I. F. David, S. R. Johnson, P. P. Edwards, P. A. Anderson, *Chem. Commun.* **2006**, 2439.
[68] P.A. Chater, W.I.F. David, P.A. Anderson, *Chem. Commun.* **2007**, 4770.
[69] G. P. Meisner, M. L. Scullin, M. P. Balogh, F. E. Pinkerton, M. S. Meyer, *J. Phys. Chem. B* **2006**, *110*, 4186.
[70] Y. E. Filinchuk, K. Yvon, G. P. Meisner, F. E. Pinkerton, M. P. Balogh, *Inorg. Chem.* **2006**, *45*, 1433.
[71] J. B. Yanga, X. J. Wang, Q. Cai, W. B. Yelon, W. J. James, *J. Appl. Phys.* **2007**, *102*, 033507.
[72] H. Wu, W. Zhou, T. J. Udovic, J. J. Rush, T. Yildirim, *Chem. Mater.* **2008**, *20*, 1245.
[73] M. Matsuo, A. Remhof, P. Martelli, R. Caputo, M. Ernst, Y. Miura, T. Sato, H. Oguchi, H. Maekawa, H. Takamura, A. Borgschulte, A. Züttel, S. Orimo, *J. Am. Chem. Soc.* **2009**, *131*, 16389.
[74] M. Matsuo, T. Sato, Y. Miura, H. Oguchi, Y. Zhou, H. Maekawa, H. Takamura, S. Orimo, *Chem. Mater.* **2010**, *22*, 2702.
[75] O. M. Løvvik, S. M. Opalka, H. W. Brinks, B. C. Hauback, *Phys. Rev. B* **2004**, *69*, 134117.
[76] P. Vajeeston, P. Ravindran, A. Kjekshus, H. Fjellvåg, *Phys. Rev. B* **2004**, *69*, 020104.
[77] M. J. van Setten, V. A. Popa, G. A. de Wijs, G. Brocks, *Phys. Rev. B* **2007**, *75*, 035204.
[78] B. C. Hauback, H. W. Brinks, H. Fjellvåg, *J. Alloys Compd.* **2002**, *346*, 184.
[79] H. W. Brinks, B. C. Hauback, *J. Alloys Compd.* **2003**, *354*, 143.
[80] H. Oguchi, M. Matsuo, T. Sato, H. Takamura, H. Maekawa, H. Kuwano, S. Orimo, *J. Appl. Phys.* **2010**, *107*, 096104.
[81] M. Menjo, H.-W. Li, M. Matsuo, K. Ikeda, S. Orimo, *J. Ceram. Soc. Japan* **2009**, *117*, 457.
[82] R. Nesper, *Prog. Solid State Chem.* **1990**, *20*, 1.

[83] M. Wörle, R. Nesper, *Z. Anorg. Allg. Chem.* **1995**, *651*, 1153.
[84] H. Rosner, A. Kitaigorodsky, W. E. Pickett, *Phys. Rev. Lett.* **2002**, *88*, 127001.
[85] A. Bharathi, S. J. Balaselvi, M. Premila, T. N. Sairam, G. L. N. Reddy, C. S. Sundar, Y. Hariharan, *Solid State Commun.* **2002**, *124*, 423.
[86] L. Zhao, P. Klavins, K. Liu, *J. Appl. Phys.* **2003**, *93*, 8653.
[87] D. Souptel, Z. Hossain, G. Behr, W. Löser, C. Geibel, *Solid State Commun.* **2003**, *125*, 17.
[88] A. M. Fogg, P. R. Chalker, J. B. Claridge, G. R. Darling, M. J. Rosseinsky, *Phys. Rev. B* **2003**, *67*, 245106.
[89] Y. Nakamori, S. Orimo, *J. Alloys Compd.* **2004**, *370*, L7.
[90] T. Hitosugi, H. Oguchi, private communication.
[91] J. Kawamura, in *Solid State Ionics for Batteries*, (Eds: T. Minami, M. Tatsumisago, M. Wakihara, C. Iwakura, S. Kohjiya, I. Tanaka), Springer-Verlag, Berlin **2005**.
[92] J. M. Donelan, Q. L. V. Naing, J. A. Hoffer, D. J. Weber, A. D. Kuo, *Science* **2008**, *319*, 807.
[93] N. E. duToit, B. L. Wardle, S. G. Kim, *Integ. Ferroelectrics* **2005**, *71*, 121.
[94] S. B. Horowitz, M. Sheplak, L. N. Cattafesta, T. Nishida, *J. Micromech. Microeng.* **2006**, *16*, S174.
[95] H. Okamoto, T. Onuki, H. Kuwano, *Appl. Phys. Lett.* **2008**, *93*, 122901.
[96] M. Armand, F. Endres, D. R. MacFarlane, H. Ohno, B. Scrosati, *Nature Mater.* **2009**, *8*, 621.
[97] D. E. Farrell, D. Shin, C. Wolverton, *Phys. Rev. B* **2009**, *80*, 224201.
[98] Y. Fukai, in *The Metal-Hydrogen System*, 2nd Ed., Springer-Verlag, Berlin **2005**.
[99] L. Pontonnier, S. Miraglia, D. Fruchart, J. L. Soubeyroux, A. Baudry, P. Boyer, *J. Alloys Comp.* **1992**, *186*, 241.
[100] W. I. F. David, M. O. Jones, D. H. Gregory, C. M. Jewell, S. R. Johnson, A. Walton, P. P. Edwards, *J. Am. Chem. Soc.* **2007**, *129*, 1594.
[101] T. Noritake, H. Nozaki, M. Aoki, S. Towata, G. Kitahara, Y. Nakamori, S. Orimo, *J. Alloys Comp.* **2005**, *393*, 264.